11th World Congress on Computational Mechanics (WCCM XI)
5th European Conference on Computational Mechanics (ECCM V)
6th European Conference on Computational Fluid Dynamics (ECFD VI)
E. Oñate, J. Oliver and A. Huerta (Eds)

APPLICATION OF COMPUTATIONAL FLUID MECHANICS FOR PROTECTION CLOTH DESIGN

Irina Cherunova*, Nikolai Kornev†, Gunnar Jacobi †, Ievgeniia Treshchun†, Andreas Gross†, Johann Turnow†, Sebastian Schreier† and Mathias Paschen†

* Don State Technical University
Shevchenko str. 147, 346500 Shakhty, Russia
e-mail: isch@mail.ru, web page: http://www.sssu.ru/

† University of Rostock
A. Einstein Str.2, 18059 Rostock, Germany
e-mail: nikolai.kornev@uni-rostock.de - Web page: http://www.lemos.uni-rostock.de

Key words: Human Thermodynamics, Conjugate Heat Transfer, Computational Fluid Dynamics, Fluid- Structure Interaction, Cloth Design

Abstract. The paper presents three samples of CFD application for design of cloth protecting from high and low temperatures with and without incident flow. Inner human body thermodynamics as well as the interaction of human body with surrounding media are considered. The inner and outer problems are treated decoupled with specific boundary conditions.

1 INTRODUCTION

Computational Fluid Dynamics is a powerfull tool with applications in a wide range of technical disciplines. Along with classical technical areas, CFD is also used increasingly for calculations of human thermodynamics and evaluation of comfort conditions [1], [2]. The aim of this paper is to make the CFD community acquainted with a relative new application area: design of clothes necessary to protect people from the action of extremely low or high temperatures with and without wind. The task can be classified as a typical problem with thermomechanical coupling of fluids (air or water) and structures (human body and clothes). The body generates the heat within certain organs which is then transferred by the thermal diffusion through the body substance possessing very non uniform properties. A large fraction of the heat generated by internal organs is transported to the body periphery by a complicated net of blood vessels. Penetrating the cloth the heat is transported away from the human by heat conduction in surrounding medium, natural and forced convection, breathing, radiation and transpiration. While a full detailed model of the human thermodynamics is still remaining the problem of the future, the practical

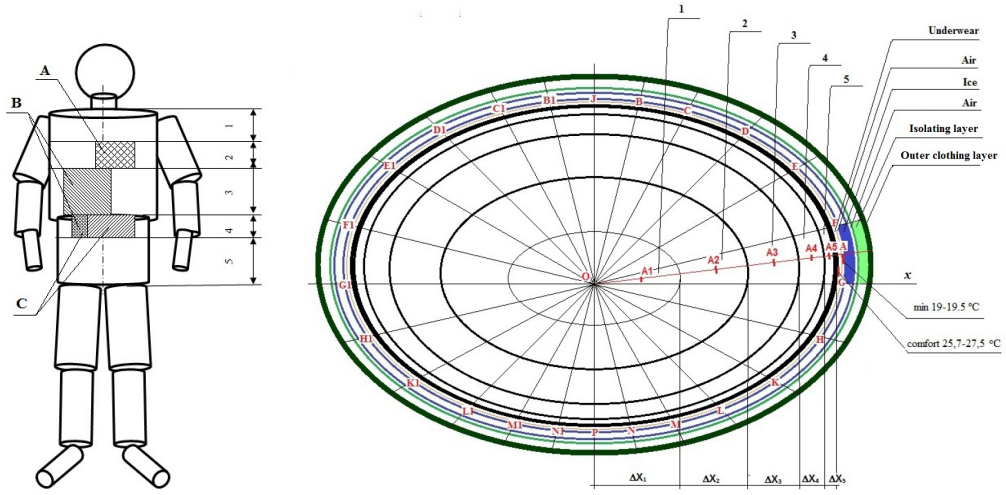

Figure 1: **Left:** Sketch of the human body used in simulations. A- heart, B- liver, C - kidney. **Right:** Horizontal cross section of the human body represented as an ellipse with five layers: 1- inner core, 2- outer core, 3- muscles, 4- fat, 5- skin.

design of protection clothes demands the reliable models already now. Such models are necessary to reduce the time and costs consuming measurements and to avoid dangerous experiments with people under emergency conditions. The paper presents a few CFD models which reflect the evolution of CFD modelling for cloth design done in our research group. Each model is built on previous ones with increase of complexity and accuracy of modelling.

2 CFD Design of cloth for protection of workers at high temperatures without wind

The coupled problem of thermomechanical interaction can be subdivided into inner (heat transfer through the body and cloth) and outer (dissipation of heat into surrounding medium) submodels. For some specific purposes they can be decoupled. The interaction is considered by formulation of proper boundary conditions.
In the most of modern inner submodels the human body is represented as a set of geometric elements according to the original idea proposed by Stolwijk. The human body is considered as a slender body with heat transfer dominating in horizontal planes neglecting the heat fluxes in the vertical direction (Fig. 1). The cross section of the body is subdivided into the five layers (Fig. 1): skin, fat layer, muscles and two core layers. The core represents all human organs and blood vessels. The cross section of the human body is then represented as a set of sectors subdivided along the radius into five layers with constant thermal properties (Fig. 1). The geometrical data, thermodynamical coefficients for diffferent parts of the human body are given in [3]. The ice and the clothes layer are modelled by additional layers covering the human body.

The natural convection in the surrounding air is neglected. The heat transfer within each horizontal plane is modelled using a simple sector model assuming, that the heat exchange between the sectors is negligible at every cross section of the human body. The heat transfer along the radius x within each sector is described by the one dimensional heat conduction equation derived from the energy conservation consideration. The change of the internal energy in the sector element with coordinates x and $x + dx$ due to heat transport within the time dt is

$$dQ_1 = \left(k(x+dx)S(x+dx)\frac{\partial T}{\partial x} - k(x)S(x)\frac{\partial T}{\partial x} \right) dt \approx \frac{\partial}{\partial x}\left(k(x)S(x)\frac{\partial T}{\partial x} \right) dt \quad (1)$$

where $T(x,t)$ is the temperature, k is the thermal conductivity, $S(x) = \alpha x h$ is the sector arc length multiplied with its height h and α is the central angle of the sector. Within the material we have additionally the heat release with the heat density F (heat per unit volume):

$$dQ_2 = SFdxdt \quad (2)$$

Due to the heat transfer and heat release the internal energy of the material is changed by dQ_3

$$dQ_3 = c_p \rho S \frac{\partial T}{\partial t} dxdt \quad (3)$$

where c_p is the specific heat capacity and ρ is the mass density of the material. By conservation of energy

$$dQ_1 + dQ_2 = dQ_3$$

or

$$S(x)\frac{\partial T}{\partial t} = \lambda \frac{\partial}{\partial x}\left(S(x)\frac{\partial T}{\partial x} \right) + S(x)f(x) \quad (4)$$

where $\lambda(x) = k/(c_p\rho)$ is the thermal diffusivity and $f(x) = F(x)/(c_p\rho)$.
The equation (4) is solved at the initial condition

$$T(x,0) = \varphi(x) \quad (5)$$

and the boundary conditions formulated at the sector center

$$T(0,t) = T_{core} \quad (6)$$

and at the outer boundary of the clothes

$$T(x_{outer},t) = T_{med} \quad (7)$$

The temperature of the surrounding medium was $T_{med} = 50^0$. It was assumed that the core center (at $x = 0$) temperature was constant in time $T_{core} = 36.7^0$.
The heat transfer process is subdivided into three steps. Within the first step the ice is warmed up to the melting temperature. The melting process is followed by the absorption of the heat coming from both the surrounding medium Q_{med}

$$\dot{Q}_{med} = \lambda_{med} \frac{\partial T}{\partial x} A_{med} \tag{8}$$

and the human body Q_{hum} caused by metabolism

$$\dot{Q}_{hum} = \lambda_{skin} \frac{\partial T}{\partial x} A_{skin} \tag{9}$$

where λ_{med} is the thermal diffusivity of the clothing layer adjacent to the ice layer, A_{med} is the surface between the ice layer and adjacent clothing layer in a sector under consideration, λ_{skin} is the thermal diffusivity of the human skin and A_{skin} is the skin surface in the sector. The second step is the ice layer melting. It is assumed that the water and ice mixture is uniform with the constant temperature of zero degrees of Celsius. The dynamics of the boundary between the water and ice is not considered. The heat fluxes (8) and (9) are constant in time. The second step is finished in time t^* once the ice is melted:

$$Q_{melt} = (\dot{Q}_{med} + \dot{Q}_{skin}) t^* \tag{10}$$

Here Q_{melt} is the heat necessary to melt the whole ice. After that, within the third step the water from the melted ice is warming up due to heat fluxes (8) and (9) continuing in time. The calculations within the third step are running as long as the comfort conditions are fulfilled.
The equation (4) is solved using the finite differential method on the uniform grid $\Delta x = const$ with the constant time step $\Delta t = const$. The numerical implementation utilizes the central differential scheme for space derivatives and Crank Nicolson implicit representation of the unsteady term. An inhouse code was developed for this purposes. The temperature at the outer boundary of cloth was specified.
This model was utilized in [3] to design special jackets made of the textile with embedded ice layer (Fig. 2, left) to protect the rescue teams working in the mining industry (Fig. 2, centre). Numerical calculations are performed with the aim to determine the ice layer thickness necessary to keep the temperature of the human body core at the temperature of $36.7^0 \pm 1^0$ within one hour. The experiments with clothes supported the simulation prediction (see Fig. 2, right) which then were used for design of protection cloth.

3 CFD Design of cloth for protection of divers at low temperatures under current conditions

Study was performed for the model Tin Man presented in Fig. 3. Inner thermodynamics in the body was not modelled. The temperature of the human body was assumed to be

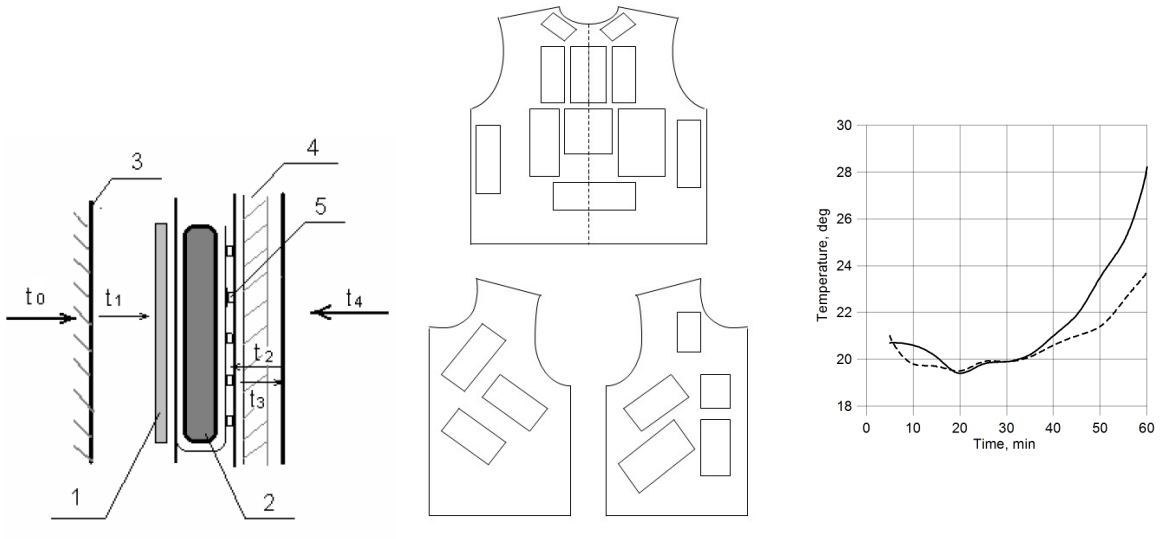

Figure 2: **Left:** Ice protection construction. 1- polyurethane foam, 2- ice briquette, 3- human body, 4- special overheating protection clothes, 5- polyurethane net (air layer). **Centre:** Overheating protection jacket designed on the base of simulations. **Right:** Development of the averaged temperature in the air gap between the underwear and the ice protection on the human chest. Comparison between the measurement (solid line) and the numerical simulations (dotted line).

constant and equal to 33^0 at the temperature of the surrounding medium of 10 degrees of Celsius. Thus, the Dirichlet boundary conditions were enforced for the temperature whereas the heat flux from the body was calculated. Heat exchange by shivering, breathing and radiation was neglected. The heat exchange between the body and surrounding medium is mostly determined by the convection due to wind. The incompressible flow was calculated using steady RANS (Reynolds Averaged Navier- Stokes Equations) using the $k-\omega$ SST model. Temperature was considered as a passive scalar determined from the temperature transport equation. The framework OpenFOAM was utilized for the numerical solution of this problem.

First, CFD was validated for the case of the air flow. Distribution of the heat transfer coefficient along the Tin Man body is shown in Fig. 3, left. The minimal heat flux takes place in the separation area with reduced flow velocities, i.e. behind the body arms and head, as well as in the stagnation area in the front part of the body. Figure 3 illustrates the integral coefficient of the heat transfer h_c obtained by integration over the whole body surface. Results of authors marked by crosses are compared with experimental data of de Dear et al. (triangles) and different calculations. Shadowed grey area shows the scattering of data otbained using various approaches. Big scattering of data illustrates the complexity of the problem of the human body thermodynamics interaction with a surrounding medium. Our results agree satisfactory with measurements. Note that the calculations at small air speeds were performed assuming the laminar character of the flow.

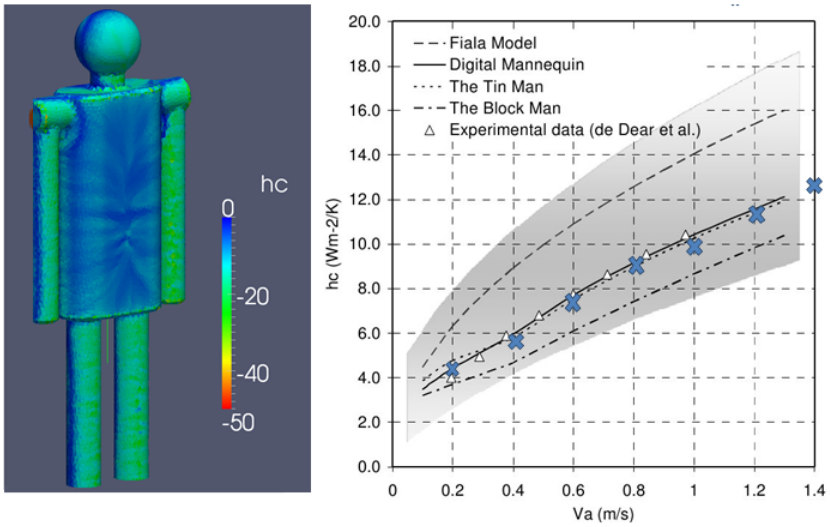

Figure 3: **Left:** Heat transfer coefficient at air speed of $1m/s$. **Right:** Whole body convective heat transfer coefficient h_c from various published works. The figure is taken from [1]. Blue crosses show results of the present work.

Within the next step the Tin Man body was weared in a neoprene cloth with the thickness of 1.0 cm to reproduce the case of a diver working at low temperatures of 10^0 in a sea current with the speed of 1 m/s. The Tin Man body temperature was uniformly distributed along the body and was 33 degrees of Celsius. The cloth was assumed to be waterproof and uniformly contaminated by oil products. This case is typical for ship repair works and rescue and technical operations in oil spill zones. Contamination in terms of gram per centimeter squared as well as the heat diffusivity coefficient of contaminated cloth are given in the table 1. The size of the computational domain was $12 \times 12 \times 6$ meters, whereas the size of the body was 1.65 meters. For discretization a mesh with 1.3 million of cells was used with y^+ values below 0.5 on the whole body. The results for heat flux depending on the contamination are presented in the last column of table 1 and in Fig. 4. As seen the heat flux is almost linear function of the contamination.
The Tin Man body is a primitive simplest geometry. From one side, it makes the solution of the inner thermodynamics problem much easier. From the other side, such simplified geometry is not suitable for aerodynamic calculations since it consists of sharp edges with numerous strong separations. Numerical solution becomes unstable leading to unsatisfactory convergence. Although the real human body is geometrically more complex, the flow around it can be calculated much easier than in the Tin Man case. Therefore, further investigations done by our group were performed for real human body geometry (Fig. 5) designed by the Hohenstein Institute [4] based on the detailed antropological study of different people categories.

Contamination g/cm^2	Heat diffusivity m^2/s	Heat flux W/m^2s
0.0	$2.07 \cdot 10^{-6}$	1.89
0.5	$2.72 \cdot 10^{-6}$	2.41
2.5	$5.27 \cdot 10^{-6}$	4.46
4.5	$7.74 \cdot 10^{-6}$	6.33
6.5	$1.01 \cdot 10^{-5}$	8.08

Table 1: Heat flux from the diver depending on the cloth contamination

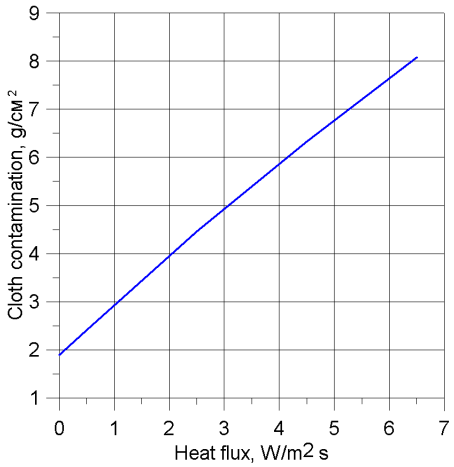

Figure 4: Heat flux from the diver depending on the cloth contamination

4 CFD application for design of cloth for protection from low temperatures under wind conditions. Influence of the wind on the cloth deformation and heat transfer from the body.

Lebedeva and Brink [5] have shown the influence of wind on heat transfer due to cloth deformation caused by wind induced pressures. Experimental study was performed in open type wind tunnel with closed test section up to Reynolds number of $3.6 \cdot 10^5$ based on the air speed and diameter of cloth packages in form of cylinders. The aim of the present work is to get similar estimations for real human body form.

4.1 Wind tunnel measurements of pressure distribution

The experiment was conducted in the wind tunnel of the Chair of Ocean Engineering at the Rostock University. The wind tunnel of the Göttingen type has the test section of lengths of 2.8 m with the square cross section of $1.4 \times 1.4\ m^2$. The model of the height of 700 mm was manufactured by downsizing the real body with the scale factor of 0.39. Within the open test section the size of the air jet with uniform velocity distribution is estimated as one meter at least. Since it is one and half times as large as the model height, the influence of the jet boundaries on flow around the body can be considered as negligible. Two measurement series were performed. In the first one the pressure was measured at nine points distributed at three cross sections $z = 0.329, 0.418$ and 0.476 (see Fig. 5 and 7) using inclined manometers which are very accurate for low pressures measurements. Due to high inertia of inclined manometers the unsteady pressure oscillations are not captured. Position of measurement points is shown in Fig. 5 (points $1, 1', 1''$, $5, 5', 5''$ and $9, 9', 9''$). The measurements were performed with the air speed of $10m/s$ at 14 degrees of Celsius. Reynolds number based on the maximum transversal body size is around $1.33 \cdot 10^5$. In the second series the measurements were performed at nine points $1, ..., 9$ shown

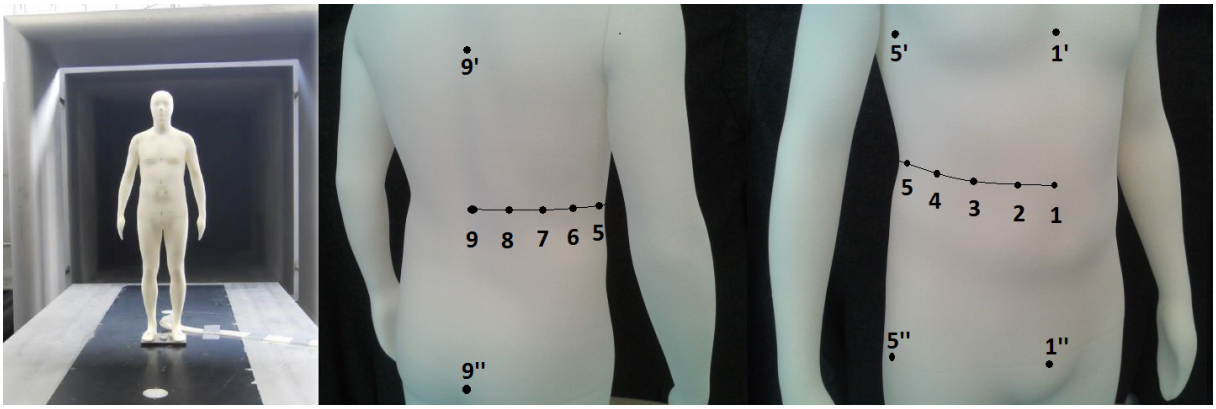

Figure 5: Human body model in wind tunnel of the Rostock university (left). Positions of measurement points (right).

in Fig. 7(right) only at $z = 0.418$ (waist). This more detailed investigation was carried out for two air speeds of 10 and 15 m/s.

4.2 Numerical simulations of pressure distribution and comparison with measurements

Numerical simulations were performed using the commercial software package STAR CCM+ for the air speed of 10 m/s. The boundary layer on the windward side is supposed to be in transitional state. Due to strong separation the flow on the leeward side of the model and in the wake can be considered as a turbulent one. The computational domain has the cross section of $2.1 \times 2.1\ m^2$. A length of the domain is 2.1 m in front of the human body (0.7 m height) and 4.2 m behind it. The grid consists of $1.2 \cdot 10^6$ polyhedron cells with maximal y^+ value of 40. On the model sides the y^+ value is varied between 20 and 25. To exclude ambiguity connected to the flow character, simulations were performed both for pure turbulent and pure laminar flows with and without roughness.

4.3 Comparison

Comparison with measurements for the first series is presented in Fig. 6. The results of measurements and simulations agree well in the front part of the body and in the separation area. Both simulations and measurements predict the increase of the pressure coefficient in the section $z = 0.476$ m at angle ≈ 90 degrees caused by the stagnation effect of the shoulder. On the side of the model in cross sections $z = 0.329$ and 0.418 the agreement is not satisfactory. To clarify this problem, the more detailed second measurement series was performed. All results obtained at $z = 0.418$ are presented in Fig. 7. The big difference takes place around the angle of approx. 90 degrees in the area of the separation (point 5 in Fig. 5). The experiment doesn't predict the strong under pressure region on the side of the model. The minimum experimental pressure coefficient is around -1 whereas the simulation predicts -2.2 both for laminar and turbulent cases.

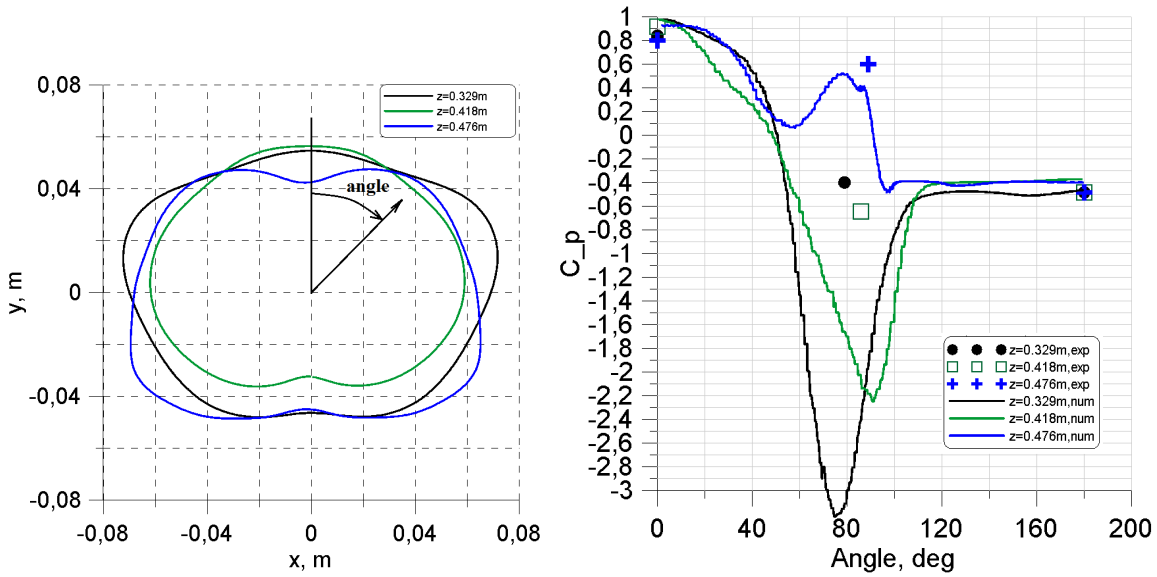

Figure 6: Contrours of torso (left) and pressure coefficient C_p distribution around the body at three different altitudes $z = 0.329, 0.418$ and 0.476m.

The difference between the laminar and turbulent solutions is negligible. This might be due to two facts. First, the cross section is elliptical (Fig. 6, left) and the averaged position of flow separation points is fixed at the widest axis and doesn't depend on the flow character. Second, strong unsteady flow oscillation makes the difference between laminar and turbulent pressure distributions negligible.

The experimental results raised many questions. Without big error, the flow can be considered as quasi two dimensional in cross sections along the human body. Then C_{pmin} is minus three for the case of two dimensional cylinder flow. Due to three dimensional effects C_{pmin} can be smaller, but not three times smaller like in measurements. The numerical simulation reveals no separation up to angle of 90 degrees. Within the separation zone at angles larger than 120 degrees the numerical pressure coefficient is nearly constant. These facts are in a good agreement with classic knowledge about bluff bodies flows. In experiment, C_p slightly increases in the separation area at angles larger than 90 degrees. Also, a relatively big discrepancy between C_p determined for 10 and 15 m/s seems to be very questionable, at least within the zone of weak Reynolds number influence, i.e. at angles less than 90 degrees. The flow at angles larger than 90 degrees is unsteady. The scattering of the data due to unsteady effects is shown both for simulations and measurement. Obviously, the unsteady pressure oscillations can not be reason for the disagreement between simulation and experiments. More detailed experimental study should be carried out in the future to clear this problem.

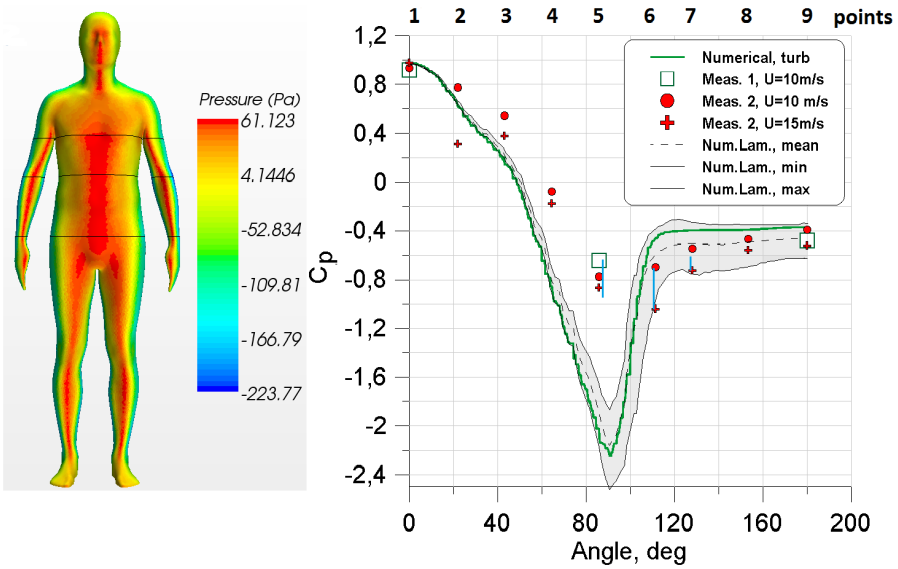

Figure 7: **Left:** Pressure distribution Δp on the body obtained using StarCCM+ commercial software. Contours of three cross sections at $z = 0.329, 0.418$ and 0.476 m are marked by black lines. **Right:** Pressure coefficient C_p distribution around the body at $z = 0.418$. Points position $1, .., 9$ is shown in Fig. 5. Grey zone is the area of unsteady pressure coefficient oscillations in the laminar solution. Vertical lines indicate the scattering of experimental data at points 5, 6 and 7.

4.4 Change of thermal conductivity caused by wind induced pressures

Estimations of pressure influence on cloth thermal conductivity was performed experimentally in the Thermal laboratory of the Don State Technical University. The cloth of 30 mm thickness was manufactured from the Saviour with Flamestat Cotton (upper sheet), the insulation Thinsulate and Taffeta as a lining. The cloth is used in oil industry for work at very low temperatures under oil contamination conditions.

It was assumed that the pressure acts only in normal direction and shear stresses are neglected. The cloth has such a structure that it can be pressed but not stretched. With the other words, the cloth has no deformation if the pressure difference $\Delta p = p - p_{atm}$ is negative. Bearing this in mind, the cloth deformation calculated using numerical pressure data can be considered as reliable one since the area of positive C_p is approximately the same in experiments and simulations. The cloth samples were subjected to pressure and then the thermal conductivity was measured using steady state method. Approximation of measurement points results in the following interpolation formula:

$$k = 0.22 + c_1 \Delta p + c_2 \Delta p^2 \tag{11}$$

where k is the thermal conductivity coefficient in W/mK, $C_1 = 9.322 \cdot 10^{-4} \frac{W}{mKPa}$ and $C_2 = 9.775 \cdot 10^{-6} \frac{W}{mKPa^2}$. Fig. 8 shows distribution of the thermal conductivity around the body at three sections along the human body. As seen the conductivity can increase in

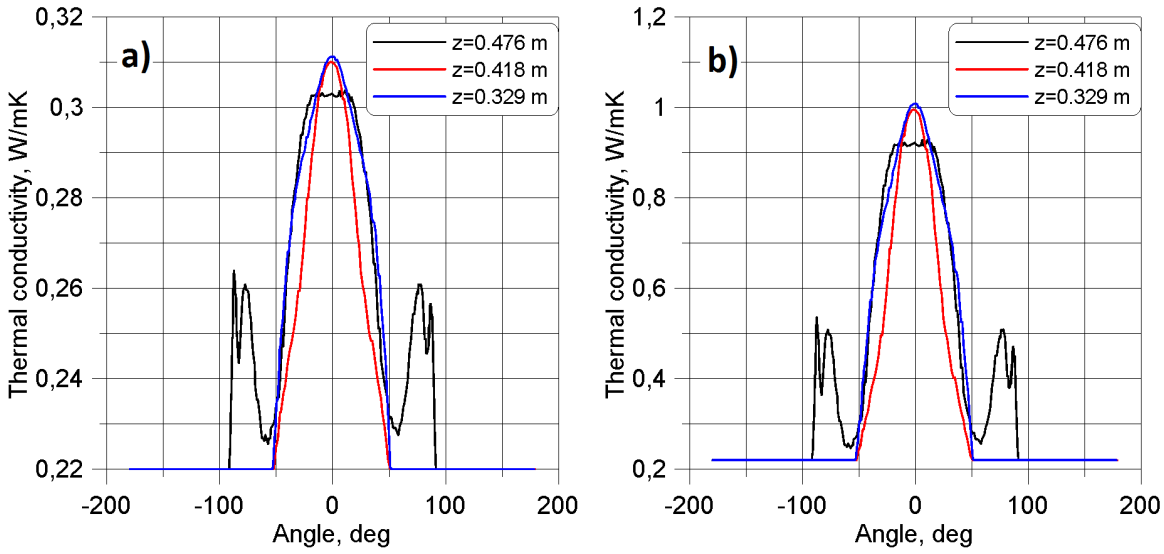

Figure 8: Change of thermal conductivity due to pressure induced by wind of 10 m/s (left) and 20 m/s (right). Thermal conductivity without wind is 0.22 W/mK.

the stagnation area at the chest up to four and half times for strong wind of 20 m/s. To estimate the integral wind influence f the thermal conductivity referred to that without wind was integrated over the body at five sections:

$$f(z) = \oint k(wind \neq 0)/k(wind = 0) r \; d\vartheta \tag{12}$$

where ϑ and r are zylindrical coordinates in a cross section. The results are summarized in the table 2. At strong wind of 20 m/s or 72 km/h the integral increase of thermal conductivity can be up to seventy percent in the chest cross section. At moderate wind of 10 m/s the maximum influence is less than ten percent.

Table 2: Thermal conductivity factor $f(z)$ integrated in circumferential direction

Body part	Wind 10 m/s	20 m/s
Chest ($z = 0.476$ m)	1.096	1.729
Waist ($z = 0.418$ m)	1.025	1.199
Hip ($z = 0.329$ m)	1.085	1.668
Upper leg ($z = 0.25$ m)	1.025	1.194
Lower leg ($z = 0.12$ m)	1.018	1.141

5 CONCLUSIONS

The paper demonstrates capabilities of CFD for design of special protection cloth. In particular, the following main results were obtained:

- The results of simulations were used for design of special overheating protection jacket with ice briquettes to prevent the body overheating and to keep the temperature of the body core at $36.7^0 \pm 1^0$ within one hour. The laboratory tests of the jacket and trials at real conditions confirmed the prediction of the numerical simulations.

- Using CFD the heat transfer between a diver dressed in a neoprene suit and cold water with current was studied to estimate the influence of cloth contamination by oil products. The heat loss is almost linear function of the contamination.

- Under strong wind conditions the heat transfer from the human body can sufficiently be increased due to change of the thermal conductivity caused by cloth deformation under wind induced pressures.

6 Acknowledgements

The first author was supported by the Russian Ministry of Education and Research, the work of the other authors was funded by the German Federal Ministry of Education and Research (BMBF) (grants 01DJ12109A and PROMOTE).

REFERENCES

[1] Y. Zhang, D. Novieto, J. Yingchun (2009). Human envoronmental heat transfer simulation with CFD- the advances and challenges. *Building Simulation 2009*, Eleventh International IBPSA Conference, Glasgow, Scotland, July 27–30, 2009, 2162–2168.

[2] J. Seo, J. Park, Y. Choi (2013). Numerical study of human model shape and grid dependency for indoor thermal comfort evaluation. *J. Mechanical Science and Technology*, **Vol. 27**, Issue 2, pp. 397-405.

[3] I. Cherunova, N. Kornev and I. Brink (2012). Mathematical model of the ice protection of a human body at high temperatures of surrounding medium, *Engineering Research*, **Vol. 76**, Issue 3, pp. 97-103.

[4] www.hohenstein.de

[5] I. Brink and E. Lebedeva (2005). Investigation of wind influence on packages of heat protecting cloth. *Textile Industry*, **Vol. 3**, pp. 34-36 (in Russian).